



**HAL**  
open science

# Two Measurement Scenarios for Anonymous Mutual Localization in Multi-UAV Systems

Marco Cognetti, Paolo Stegagno, Antonio Franchi, Giuseppe Oriolo

► **To cite this version:**

Marco Cognetti, Paolo Stegagno, Antonio Franchi, Giuseppe Oriolo. Two Measurement Scenarios for Anonymous Mutual Localization in Multi-UAV Systems. IFAC Proceedings Volumes, 2012, 45 (28), pp.13-18. 10.3182/20121003-3-SF-4024.00006 . hal-04287193

**HAL Id: hal-04287193**

**<https://hal.science/hal-04287193>**

Submitted on 15 Nov 2023

**HAL** is a multi-disciplinary open access archive for the deposit and dissemination of scientific research documents, whether they are published or not. The documents may come from teaching and research institutions in France or abroad, or from public or private research centers.

L'archive ouverte pluridisciplinaire **HAL**, est destinée au dépôt et à la diffusion de documents scientifiques de niveau recherche, publiés ou non, émanant des établissements d'enseignement et de recherche français ou étrangers, des laboratoires publics ou privés.

# Two Measurement Scenarios for Anonymous Mutual Localization in Multi-UAV Systems

Marco Cagnetti\* Paolo Stegagno\* Antonio Franchi\*\*  
Giuseppe Oriolo\*

\* *DIAG, Università di Roma La Sapienza, Rome, Italy*

(*e-mail: marco.cagnetti@gmail.com, {stegagno,oriolo}@dis.uniroma1.it*).

\*\* *Max Planck Institute for Biological Cybernetics, Tübingen, Germany*

(*e-mail: antonio.franchi@tuebingen.mpg.de*)

---

**Abstract:** We present a method for reconstructing the relative poses among the components of a multi-UAV system using anonymous (i.e., without identity information) robot-to-robot measurements. We consider two cases: bearing-only and bearing+distance measurements. While bearing can be rather directly extracted from a camera image, visual reconstruction of distances is more elaborate and typically associated with a larger noise. Nevertheless, our experiments show that use of such metric information improves significantly the quality of the localization.

*Keywords:* Localization, anonymous measurements, 3-D environment, multi-UAV.

---

## 1. INTRODUCTION

Knowing relative poses among the members of a multi-robot system is essential whenever the task requires some form of cooperative perception or motion coordination. By attaching to each robot a (moving) frame, one may define *Relative Mutual Localization* (RML) as the problem of maintaining an accurate estimate of the transformations among the various robot frames using robot-to-robot measurements. This topic has been thoroughly studied in 2-D environments (Fox et al., 2000; Roumeliotis and Bekey, 2002; Howard et al., 2002). Recently, due to the growing interest in multi-UAV systems, the 3-D case has been considered; for example, Zhou and Roumeliotis (2011) find the minimal sets of data needed to compute 3-D relative poses, while Trawny et al. (2010) and Martinelli (2012) have proposed specific estimators.

All the above works assume that the robot-to-robot measurements come with the identity of the measured robot. However, to achieve this, the robots should preliminarily agree on some form of individual tagging. An alternative, more decentralized scenario is to address the RML problem using *anonymous* measurements. This situation, in which the data association of the measures is unknown, was first considered for 2-D RML with position measurements (Franchi et al., 2009, 2010), and later extended to 2-D and 3-D RML with bearing-only measurements (Stegagno et al., 2011; Cagnetti et al., 2012).

In 3-D environments, robot-to-robot measurements are typically obtained from on-board cameras. In particular, robot-to-robot bearing can be continuously measured by tracking one or more features associated to the ‘other’ robot in the image stream and using simple geometry. In principle, from the same sensory equipment one can

also reconstruct the robot-to-robot distance, e.g., by using image moments related to the area of the robot image. Clearly, distance measurements will be affected by larger levels of noise with respect to bearing measurements.

The objective of this paper is to consider two different scenarios for 3-D anonymous mutual localization, i.e., the use of bearing-only vs. bearing+distance measurements. The problem formulation is given in Sect. 2. A localization system that works for both scenarios, and generalizes the bearing-only case proposed in Cagnetti et al. (2012), is described in Sect. 3. Comparative experimental results obtained with a quadrotor team are shown in Sect. 4.

## 2. PROBLEM FORMULATION

Throughout this section, refer to Fig. 1 for illustration. Consider a system of  $n$  robots  $A_1, \dots, A_n$ , with  $n$  unknown and variable during operation. Each  $A_i$  is a rigid body moving in  $\mathbb{R}^3$  equipped with a body frame  $\mathcal{B}_i : \{O_{\mathcal{B}_i}, X_{\mathcal{B}_i}, Y_{\mathcal{B}_i}, Z_{\mathcal{B}_i}\}$  attached to its center of mass, defined according to the North-East-Down (NED) convention, as common in the aerospace field. Denoting by  $\mathcal{W} : \{O_{\mathcal{W}}, X_{\mathcal{W}}, Y_{\mathcal{W}}, Z_{\mathcal{W}}\}$  an inertial world frame, the configuration of  $A_i$  is described by the position  ${}^{\mathcal{W}}p_{\mathcal{B}_i} \in \mathbb{R}^3$  of the origin  $O_{\mathcal{B}_i}$  of  $\mathcal{B}_i$  in  $\mathcal{W}$  and by the rotation matrix  ${}^{\mathcal{W}}R_{\mathcal{B}_i} \in SO(3)$  between  $\mathcal{W}$  and  $\mathcal{B}_i$ . Denoting with  $R_X(\cdot)$ ,  $R_Y(\cdot)$ , and  $R_Z(\cdot)$  the canonical rotation matrices about the axes  $x$ ,  $y$ , and  $z$  respectively, we can write  ${}^{\mathcal{W}}R_{\mathcal{B}_i} = R_Z(\psi_{\mathcal{B}_i})R_Y(\theta_{\mathcal{B}_i})R_X(\phi_{\mathcal{B}_i})$ , where  $\psi_{\mathcal{B}_i}$ ,  $\theta_{\mathcal{B}_i}$ ,  $\phi_{\mathcal{B}_i} \in \mathbb{S}^1$  are the roll, pitch, and yaw angles of  $A_i$  respectively.

Being interested in the RML problem, we define the relative quantities  ${}^{\mathcal{B}_i}p_{\mathcal{B}_j} = {}^{\mathcal{W}}R_{\mathcal{B}_i}^T ({}^{\mathcal{W}}p_{\mathcal{B}_j} - {}^{\mathcal{W}}p_{\mathcal{B}_i})$  and  ${}^{\mathcal{B}_i}R_{\mathcal{B}_j} = {}^{\mathcal{W}}R_{\mathcal{B}_i}^T {}^{\mathcal{W}}R_{\mathcal{B}_j}$  and denote by  ${}^{\mathcal{B}_i}x_{\mathcal{B}_j} = \{{}^{\mathcal{B}_i}p_{\mathcal{B}_j}, {}^{\mathcal{B}_i}R_{\mathcal{B}_j}\}$  the *full relative pose* between  $A_i$  and  $A_j$ .

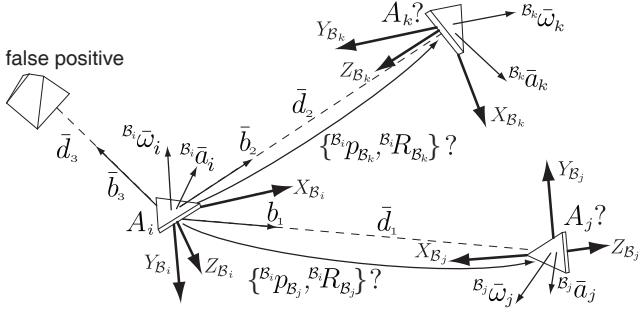


Fig. 1. Problem setting: robots (triangles) are shown with their attached frame and IMU measurements. Robot  $A_i$  detects two actual robots whose identities are unknown plus one false positive, resulting in three anonymous measurements.

Each robot  $A_i$  is equipped with a *motion detector*, such as an Inertial Measurement Unit (IMU), that provides measurements  ${}^{B_i}\bar{a}_i$ ,  ${}^{B_i}\bar{\omega}_i$  of its own acceleration  ${}^{B_i}a_i$  and angular velocity  ${}^{B_i}\omega_i$  in its body frame.

In addition,  $A_i$  comes with a *robot detector*, a sensor device which detects other robots and returns an anonymous measurement  ${}^{B_i}\bar{b}_{B_j}$  of their *relative bearing*

$${}^{B_i}\bar{b}_{B_j} = {}^{\mathcal{W}}R_{B_i}^T \frac{{}^{\mathcal{W}}p_{B_j} - {}^{\mathcal{W}}p_{B_i}}{\|{}^{\mathcal{W}}p_{B_j} - {}^{\mathcal{W}}p_{B_i}\|} \in \mathbb{S}^2 \quad (1)$$

that is, the unit-norm vector in  $\mathbb{R}^3$  pointing toward  $O_{B_j}$ , expressed in  $B_i$ . The measurement  ${}^{B_i}\bar{b}_{B_j}$  is available whenever  ${}^{B_i}p_{B_j} \in D_p$ , the *perception set* attached to the robot.

In addition to being subject to false positives (due to objects that look like robots) and false negatives (due to occlusions), relative measurements do not contain the identity of the measured robots (see Fig. 1). Therefore, the output of the robot detector is a set of measurements whose ordering has no relation to the robot indexing; in addition, each measurement may or not refer to an actual robot. For this reason, in the following, relative measurements will be generically referred to as *features*.

The robot detector can be implemented, for example, by tracking one or more features associated to other robots in the image stream of an on-board camera and using simple geometry. With the same equipment, however, one may also reconstruct robot-to-robot distances, e.g., by using image moments related to the area of the robot image. Hence, in addition to the relative bearing  ${}^{B_i}\bar{b}_{B_j}$  we may also have the *relative distance*:

$${}^{B_i}d_{B_j} = \|{}^{\mathcal{W}}p_{B_i} - {}^{\mathcal{W}}p_{B_j}\|_2 \in \mathbb{R}. \quad (2)$$

Conceivably, distance measurements reconstructed with such a procedure will be affected by a consistent level of noise. One may therefore wonder whether to use or not this information in a mutual localization scheme. To answer this question, we consider throughout the paper two different scenarios:

**Scenario I** (bearing-only): the output of the robot detector is a set  $B_{B_i}$  of bearing measurements. This scenario has already been addressed in Cognetti et al. (2012);

**Scenario II** (bearing+distance): the output of the robot detector is a set  $C_{B_i}$  of bearing+distance measurements,

with the uncertainty on the distance much larger than the uncertainty on the bearing.

Each robot is also equipped with a *communication module* that can send/receive data to/from any other robot contained in a *communication set*  $D_c$  around itself. Denote with  $N_i$  the *neighbors* of  $A_i$ , i.e., the set of robots from which  $A_i$  is receiving communication. Each message by  $A_i$  contains: (1) the robot signature (index  $i$ ), (2) the transformed acceleration measurement  $\hat{a}_i$ , (3) the transformed feature set  $\hat{B}_i/\hat{C}_i$ , and (4) the partial estimates  $\hat{\phi}_{B_i}$ ,  $\hat{\theta}_{B_i}$ ,  $\hat{\psi}_i$  (these quantities are defined in Sect. 3).

We consider the relative localization problem from the viewpoint of the generic robot  $A_i$ . In a probabilistic framework, the generic robot  $A_i$  should compute its belief about the relative poses of robots that are or have been its neighbors, using inertial and relative measurements coming from its own sensory equipment or obtained via communication. The problem can be formally stated as:

*Problem 1.* For  $t = 1, 2, \dots$  and  $j \in N_i^{1:t}$ , compute the *belief*:

$$\text{bel}({}^{B_i}x_{B_j}) = P({}^{B_i}x_{B_j}^t | {}^{B_i}\bar{a}_i^{1:t}, {}^{B_i}\bar{\omega}_i^{1:t}, I_{B_i}^{1:t}, \{{}^{B_j}\bar{a}_j^\tau, {}^{B_j}\bar{\omega}_j^\tau, I_{B_j}^\tau\}_{j \in N_i^\tau, \tau=1, \dots, t})$$

with

$$I_{B_j}^\tau = \begin{cases} B_{B_j}^\tau & \text{in Scenario I} \\ C_{B_j}^\tau & \text{in Scenario II} \end{cases}$$

Superscripts  $t$  and  $1:t$  denote the value of a variable at time  $t$  and the history of its values at times  $1, 2, \dots, t$ .

### 3. THE MUTUAL LOCALIZATION SYSTEM

Denote with  $C_i : \{O_{C_i}, X_{C_i}, Y_{C_i}, Z_{C_i}\}$  the frame having the same origin of  $B_i$  and such that  ${}^{\mathcal{W}}R = R_Z(\psi_{B_i})$ , so  ${}^{C_i}R_{B_i} = R_Y(\theta_{B_i})R_X(\phi_{B_i})$ . Note that the  $XY$  planes (as well as the  $Z$  axes) of the reference frames  $\mathcal{W}$ ,  $C_i$ ,  $i = 1, 2, \dots, n$  are parallel to each other. Using  $C_i$  allows to split Problem 1 in two subproblems (see Fig. 2).

First,  $A_i$  estimates its roll and pitch angles ( $\phi_{B_i}$  and  $\theta_{B_i}$ ) using a complementary filter based on the IMU measurements  ${}^{B_i}\bar{a}_i$  and  ${}^{B_i}\bar{\omega}_i$  (Mahony et al., 2008). Then, using this information,  $A_i$  produces an estimate  ${}^{C_i}\hat{R}_{B_i} = R_Y(\hat{\theta}_{B_i})R_X(\hat{\phi}_{B_i})$  of  ${}^{C_i}R_{B_i}$ .

Second,  $A_i$  solves a simpler problem with respect to Problem 1, consisting in retrieving the identities of the measurements and estimating a reduced relative pose  ${}^i x_j = \{{}^i p_j, {}^i R_j\}$ ,  $j \in N_i$ , where

$${}^i p_j = {}^{\mathcal{W}}R_{C_i}^T ({}^{\mathcal{W}}p_{C_j} - {}^{\mathcal{W}}p_{C_i})$$

$${}^i R_j = R_Z(\psi_{B_i})^T R_Z(\psi_{B_j})$$

Denote by  ${}^i \hat{x}_j = \{{}^i \hat{p}_j, {}^i \hat{R}_j\}$  the corresponding estimates.

When both subproblems are solved, the estimate of  ${}^{B_i}x_{C_i}$  can be computed as  ${}^{B_i}\hat{x}_{B_j} = \{{}^{B_i}\hat{p}_{B_j}, {}^{B_i}\hat{R}_{B_j}\}$ , where  ${}^{B_i}\hat{p}_{B_j} = {}^{C_i}\hat{R}_{B_i}^T {}^i \hat{p}_j$  and  ${}^{B_i}\hat{R}_{B_j} = {}^{C_i}\hat{R}_{B_i}^T {}^i \hat{R}_j$ .

In the estimation of the reduced relative pose  ${}^i x_j$ , instead of the motion and robot detector measurements we use the corresponding quantities in  $C_i$ , computed using the roll and pitch estimates from the complementary filter:

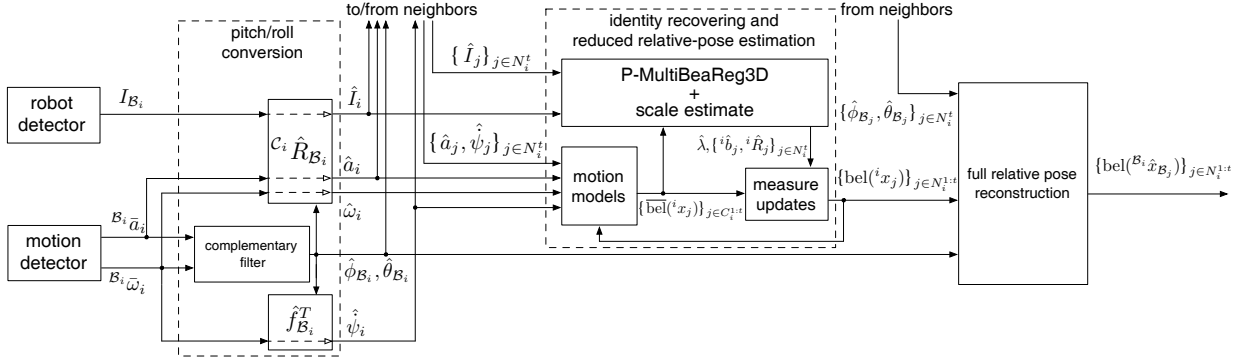


Fig. 2. Scheme of the mutual localization system that runs on the generic robot  $A_i$

$$\begin{aligned}\hat{a}_i &= C_i \hat{R}_{B_i} (0 \ 0 \ B_i \bar{a}_{i,z})^T \\ \hat{\omega}_i &= C_i \hat{R}_{B_i} (0 \ 0 \ B_i \bar{\omega}_{i,z})^T \\ \hat{b}_j &= C_i \hat{R}_{B_i} B_i \bar{b}_j\end{aligned}$$

while the distance measurements  ${}^i \bar{d}_j$  are invariant w.r.t. rotations. Note that  $\hat{a}_i$  and  $\hat{\omega}_i$  are computed using only the  $z$  component of the respective vectors, implicitly neglecting the first two components. We need to take this approximation in order to preserve the independence of the measurements and to avoid to use twice the  $x$  and  $y$  components of  $B_i \bar{a}_i$  and  $B_i \bar{\omega}_i$ , since they have already been used to compute the estimates of roll and pitch. For example, in a typical quadrotor this approximation can be safely taken assuming that the linear velocities are less than 5 m/s and the roll and pitch angles are less than  $25^\circ$  Martin and Salaün (2010). More in general, an independent source should be used, either a different sensor or a model-based prediction.

Moreover, the system uses an estimate  $\hat{\psi}_{B_i}$  of the yaw rate:

$$\hat{\psi}_{B_i} = \begin{pmatrix} 0 & \frac{\sin \hat{\phi}_{B_i}}{\cos \hat{\theta}_{B_i}} & \frac{\cos \hat{\phi}_{B_i}}{\cos \hat{\theta}_{B_i}} \end{pmatrix} B_i \bar{\omega}_i = f_{B_i}^T B_i \bar{\omega}_i. \quad (3)$$

Wrapping up, the second subsystem addresses the following simplification of Problem 1.

*Problem 2.* For  $t = 1, 2, \dots$  and  $j \in N_i^{1:t}$ , compute the belief:

$$\text{bel}({}^i x_j) = P({}^i x_j^t | \hat{a}_i^{1:t}, \hat{\omega}_i^{1:t}, \hat{I}_i^{1:t}, \hat{\psi}_i^{1:t}, \{\hat{a}_j^\tau, \hat{I}_j^\tau, \hat{\psi}_j^\tau, \}_{j \in N_i^\tau, \tau=1, \dots, t})$$

with

$$\hat{I}_j^\tau = \begin{cases} \hat{B}_j^\tau & \text{in Scenario I} \\ \hat{C}_j^\tau & \text{in Scenario II} \end{cases}$$

To solve Problem 2, the subsystem must recover: (1) the identities of measurements in  $\hat{I}_i$  and  $\hat{I}_j$  (2) the relative orientations  ${}^i R_j$  (3) the relative distances  ${}^i d_j$ . To this end, we adopt a two-step approach. First, we use a multiple registration algorithm to retrieve the identities of the measurements and the  ${}^i R_j$  matrices. Then, its output is used to feed a bank of Particle Filters (PF), one for each  $A_j, j \in N_i^{1:t}$ , to filter out the noise. In Scenario I the PFs also retrieve the scale of the formation, whereas in Scenario II this is done at the end of the multiple registration, based on distance measurements.

### 3.1 Multiple Registration Algorithm

*Registration* is the process of computing the relative poses between different viewpoints of the same scene. In Scenario I the ‘scene’ consists only of bearing measurements, and thus the scale of the relative poses cannot be recovered. In particular, given the sets of features  $\hat{B}_i, \{\hat{B}_j\}_{j \in N_i}$  and the current beliefs  $\{\text{bel}({}^i x_j)\}_{j \in N_i}$  (see Fig. 2), P-MultiBeaReg3D derives a set of guesses for the relative bearing-orientation ( ${}^i \hat{b}_j$  and  ${}^i \hat{R}_j$ ) of  $A_j, j \in N_i$ , w.r.t.  $A_i$ .

In Scenario II, the algorithm can retrieve an estimate  ${}^i \hat{d}_j$  of the distances through the  ${}^i \bar{d}_j$  measurements. Thus its output for each  $A_j$  is a set of guesses for the reduced poses  ${}^i \hat{x}_j$ . However, being the  ${}^i \bar{d}_j$ 's affected by consistent noise, we chose not to use them for recovering the identities. So, the algorithm is similar to that developed for Scenario I, with some adaptation to be discussed in Sect. 3.2. We illustrate the steps of the algorithm through the example in Fig. 3.

1) *Azimuth/Zenith-Distance representation:* Consider the situation in Fig. 3a, where four robots are arranged in a ‘square’ formation with the opposite vertices at the same height and the corresponding feature sets in Fig. 3b. Each bearing can be represented by an azimuth  ${}^i \alpha_j$  and zenith-distance  ${}^i \zeta_j$  pair, i.e.,  ${}^i b_j$  can be represented as  $({}^i \alpha_j, {}^i \zeta_j) \in [0, 2\pi) \times [0, \pi)$ , since  ${}^i b_j = (\sin {}^i \zeta_j \cos {}^i \alpha_j \ \sin {}^i \zeta_j \sin {}^i \alpha_j \ \cos {}^i \zeta_j)^T$ . The projection of  $\hat{B}_i$  on the  $XY$  plane of  $C_i$  preserves only the azimuth. Furthermore, each pair of azimuth angles in the same feature set (i.e., belonging to the same robot) can be equivalently represented by their difference. Then, an azimuth angle difference represents an internal angle of a planar triangle.

2) *Triangle finding:* Consider a triplet of robots that ‘see’ each other, e.g.,  $A_i, A_j, A_k$ , and neglect for a moment  $A_h$ , so that each robot in the triplet sees only two features, or equivalently one difference angle. Since the projection of a 3-D triangle on  $C_i$ 's  $XY$  plane defines a planar triangle, the sum of the three difference angles must be  $\pi$ . The algorithm scans all the possible triplets coming from different feature sets and looks for triplets of difference angles (one from each feature set) whose sum is  $\pi$ , with a certain tolerance. Each of these triplets defines a planar triangle up to a scaling factor. Note that a triangle encodes the identity of the robots at its vertices. Such triangles must satisfy an additional condition. Since each azimuth

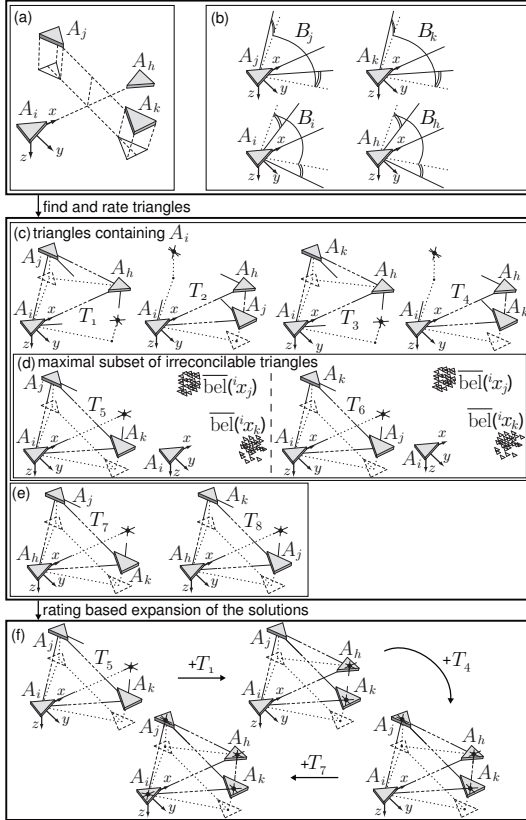


Fig. 3. Execution of P-MultiBeaReg3D in an ambiguous situation: (a) actual configuration (b) initial feature sets (c) triangle found in the first step containing the owner of the algorithm and their 2-intersections (d) maximal subset of irreconcilable triangles and their comparison with the current belief (e) other triangles found in the first step of the algorithm (f) expansion of the solution using the remaining triangles.

angle comes with a zenith-distance angle associated, by building the triangle as explained we are implying that a certain feature of a set is the equivalent of another feature of another set. Then, the sum of the zenith-distances of two associated bearings must be  $\pi$ , with a certain tolerance.

3) *2-intersections rating*: When two robots in a triangle see another robot that is not the third vertex of the triangle, their feature sets will contain two intersecting rays, one for each set. We will call this a *2-intersection*. A triangle can also have *3-intersections*, when all three robots forming it see a fourth robot (e.g.,  $A_h$  in Fig. 3a). In general, an  $n$ -intersection, that is,  $n$  intersecting rays from  $n$  different robots, accounts for  $n!/2(n-2)! = n(n-1)/2$  2-intersections. Hence, the algorithm rates all the triangles by counting their 2-intersections and collects those above a certain threshold in a set  $\mathcal{T}$  (Fig. 3c-e).

4) *Irreconcilable triangles*: The algorithm extracts from  $\mathcal{T}$  a maximal subset  $\mathcal{T}_{irr}$  (Fig. 3d) of irreconcilable triangles containing  $A_i$ ; two triangles are said to be *irreconcilable* if they associate the same robot to different features of the same set (e.g.,  $A_j$  in  $T_5$  and  $T_6$ ), or different robots to the same feature (e.g.,  $A_j$  and  $A_k$  in  $T_5$  and  $T_6$ ).

5) *Belief rating*: The triangles in  $\mathcal{T}_{irr}$  are validated (Fig. 3d) on the basis of the current belief about the pose of the

robots. To this end, we use the metric function

$$P(\{\hat{b}_j, \hat{R}_j\}) = \int p(\{\hat{b}_j, \hat{R}_j | x_j\}) \overline{\text{bel}}(x_j) d^i x_j \quad (4)$$

where  $\overline{\text{bel}}(x_j)$  comes from the particle filters. First, the scale of each triangle is calculated so as to maximize this function; then, an adaptive thresholding of these maximum values is used to select the triangles that better fit the belief. Those triangles are collected in a set  $\mathcal{T}_{best}$ .

6) *Partial solutions*: Each triangle of  $\mathcal{T}_{best}$  is the base of a branch of the algorithm and constitutes the partial solution at the first step of its branch. Let  $S$  be the partial solution of a branch at a given step;  $S$  includes (1) a collection of triangles (2) the change of coordinates between them (3) the total number of 2-intersections. In Fig. 3f the only branch has  $T_5$  as first partial solution.

7) *Iterative expansion*: The partial solution of each branch is iteratively expanded looking for triangles that have common edges with it (see Fig. 3f). Let  $\mathcal{T}_S = \{T_m, m = 1, \dots, M\}$  be the set of triangles  $T_m \in \mathcal{T}$  not yet in  $S$  having a common edge with one triangle in  $S$ . Then the algorithm builds a set of  $M$  possible partial solutions for the next step expanding  $S$  with  $T_m, m = 1, \dots, M$ . Each solution is then rated counting out its total number of 2-intersections. As in the case of the triangles, among the best rated partial solutions of each branch the algorithm selects a maximal subset of irreconcilable solutions. Among those, only the solutions that fit with the current belief according to equation (4) are used as partial solutions at following step, expanding a branch for each of them.

In the case of Fig. 3f, the algorithm expands a partial solution by joining to the triangle  $T_5$  the triangles  $T_1, T_4, T_7$  respectively at the first, second and third iteration.

The iterative process continues in each branch until  $\mathcal{T}_S$  becomes empty in that branch. In the end, each branch finds a solution, and the best of them are selected, again with the 2-intersection and belief criteria. Since each branch of the algorithm may in principle produce a different pair  ${}^i \hat{b}_k, {}^i \hat{R}_k$  for each  $A_k$ , each with its own weight, the result is a list of such pairs for the generic robot  $A_k$ .

### 3.2 Scale estimate using the distance measurements

As stated before, each branch of the algorithm finds a formation up to an unknown scaling factor  $\lambda$ . The knowledge of just one distance in the formation would be enough to produce an estimate of  $\lambda$ , hence of the whole formation. However, the high level of noise affecting the distance measurements associated to the bearing measurements in Scenario II discourages their usage in this way.

However,  ${}^i \bar{d}_j$  can be thought of as a measurement of  $\lambda$ . In this sense, each  ${}^i \bar{b}_j$  comes with an associated measurement  ${}^i \bar{\lambda}_j$ . Hence, a more accurate estimate is

$$\hat{\lambda} = \frac{\sum_{\{i,j\}} {}^i \bar{\lambda}_j \sigma_{d_{ij}}}{\sum_{\{i,j\}} \sigma_{d_{ij}}}$$

where  $\sigma_{d_{ij}}$  is the standard deviation of the noise on  ${}^i \bar{d}_j$ . Since each triangle includes at least 6 bearing measurements, even the scaling factor of a formation with few robots can be estimated quite accurately.

This estimate of  $\lambda$  is used twice in the algorithm: at the end of the algorithm to estimate the scale, and in the step of validation through the belief, where we use the estimated scale of each partial solution instead of the scale that maximizes the equation (4).

### 3.3 Filtering

The generic  $A_i$  runs one particle filter (PF $_j$ ) for each  $A_j$  to fuse the estimates coming from P-MultiBeaReg3D with the metric informations provided by the IMUs of  $A_i$  and  $A_j$ . While in Scenario II the PF needs only to filter the noise, in Scenario I it is in charge of retrieving the distances between the robots. In both cases, the use of separate beliefs  $P({}^i\chi_j)$  instead of a single joint belief  $P(\{{}^i\chi_j\}_{j \in N_i^{1:t}})$  is based on the independence assumption  $P(\{{}^i\chi_j\}_{j \in N_i^{1:t}}) = \prod_{j \in N_i^{1:t}} P({}^i\chi_j)$ . This is true in a pure localization scenario, while in certain situations it is only an acceptable approximation. In any case,  $P(\{{}^i\chi_j\}_{j \in N_i^{1:t}})$  cannot be maintained, as the dimension of its distribution grows exponentially with the number of robots. Observability of the system is guaranteed by Martinelli (2012).

The equations of motion of the system are

$${}^i\dot{p}_j = {}^i v_j \quad (5)$$

$${}^i\dot{\psi}_j = {}^i R_j a_j - a_i + [\omega_i]_{\times} {}^i v_j \quad (6)$$

$${}^i\dot{R}_j = ({}^i R_j [\omega_j]_{\times} - [\omega_i]_{\times}) {}^i R_j \quad (7)$$

where  ${}^i v_j$  is the velocity of  $O_{C_j}$  in  $\mathcal{C}_i$  and

$$[\omega_i]_{\times} = \begin{pmatrix} 0 & -\omega_{iz} & \omega_{iy} \\ \omega_{iz} & 0 & \omega_{ix} \\ \omega_{iy} & -\omega_{ix} & 0 \end{pmatrix}.$$

Since

$${}^i R_j = R_Z(-\psi_{B_i}) R_Z(\psi_{B_j}) = R_Z(\psi_{B_j} - \psi_{B_i}), \quad (8)$$

we can replace (7) with

$${}^i\dot{\psi}_j = \dot{\psi}_{B_j} - \dot{\psi}_{B_i} = f_{B_j}^T {}^{B_j} \omega_j - f_{B_i}^T {}^{B_i} \omega_i, \quad (9)$$

with  ${}^i\psi_j = \psi_{B_j} - \psi_{B_i}$  and  $f_{B_j}^T, f_{B_i}^T$  defined by (3), and compute  ${}^i R_j$  in (6) from (8). The state of each particle in PF $_j$  is the 7-tuple  ${}^i\chi_j = ({}^i p_j, {}^i v_j, {}^i\psi_j) \in \mathbb{R}^3 \times \mathbb{R}^3 \times \mathbb{S}^1$ .

The motion update step of PF $_j$  is obtained by plugging  $\hat{a}_i, \hat{a}_j, \hat{\omega}_i, \hat{\psi}_{B_i}, \hat{\psi}_{B_j}$  in (5–9). The new state probability is predicted through the integration of the motion measurements with the knowledge of the measurement noise.

As for the measurement update, P-MultiBeaReg3D may return more than one solution per robot (i.e., more than one pair  ${}^i\hat{b}_j, {}^i\hat{R}_j$ ), each solution rated on the basis of its uncertainty during the registration steps. Hence, each solution is approximated in PF $_j$  as a gaussian measurement with a covariance proportional to its uncertainty. The measurement model is given by the normalized sum of gaussians centered at the solutions of P-MultiBeaReg3D.

Denote with  ${}^i\hat{\psi}_j$  the estimate of  ${}^i\psi_j$  obtained from  ${}^i\hat{R}_j$ . The measurement update produces a rating of the predicted particles by using Bayes' law

$$P({}^i\chi_j | {}^i\hat{b}_j, {}^i\hat{\psi}_j) = N P({}^i\hat{b}_j, {}^i\hat{\psi}_j | {}^i\chi_j) P({}^i\chi_j),$$

where  $N$  is a normalization factor.

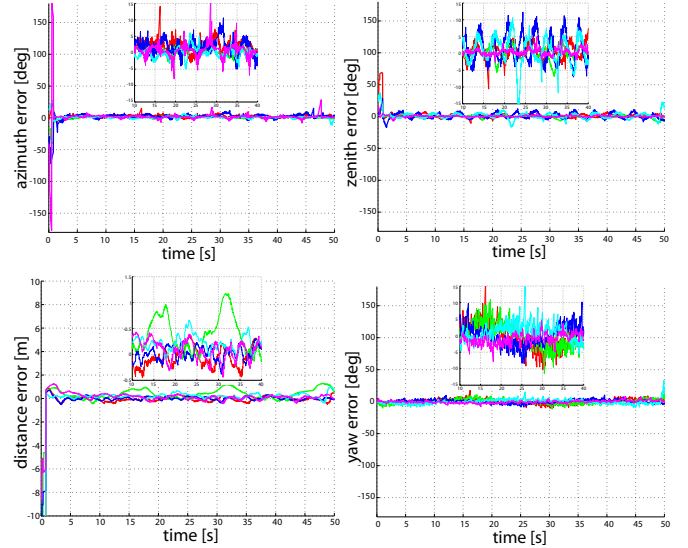


Fig. 4. Bearing-only algorithm. Errors on azimuth, zenith, distance and yaw estimates for  $A_2, \dots, A_6$  computed by  $A_1$ , with a zoom for [10, 40] s.

In Scenario II, the only difference is in the measurement update, since P-MultiBeaReg3D returns also an estimate  $\hat{\lambda}$  of the scaling factor. The resulting update law is

$$P({}^i\chi_j | {}^i\hat{b}_j, {}^i\hat{\psi}_j, \hat{\lambda}) = N P({}^i\hat{b}_j, {}^i\hat{\psi}_j, \hat{\lambda} | {}^i\chi_j) P({}^i\chi_j).$$

## 4. EXPERIMENTAL RESULTS

The mutual localization system has been tested off-line using the data collected by an 8-quadrotor team. Ground truth is provided by an external motion capture system.

The IMU mounted on the microcontroller board is used as motion detector. The microcontroller acquires data from the IMU with at 400 Hz and estimates on-line, at the same rate, the attitude of the robot through the complementary filter. An analysis on the estimates produced by the complementary filter shows a mean error of  $1.92^\circ$  for roll and  $2.67^\circ$  for pitch. However, the microcontroller can neither process nor store mutual localization data, so it sends  ${}^{B_i} \bar{a}_i, {}^{B_i} \bar{\omega}_i, \hat{\phi}_{B_i}, \hat{\theta}_{B_i}$  to a GNU-Linux machine through a serial connection with 20 Hz average rate and 4 ms standard deviation. Hence, IMU readings and attitude estimates are available at 20 Hz instead of the nominal 400 Hz, leading to a much higher noise level in the update step of the PFs.

The robot detector is analytically emulated computing  ${}^i b_j$  and  ${}^i d_j$  from the measures of the motion capture system using equations (1-2). A zero-mean gaussian noise is added to the measurements, with  $\sigma_b = 5^\circ$  standard deviation for the bearings while we have tried different values (0.3–1.5 m) for the standard deviation  $\sigma_d$  of the noise on the distances. False negatives are randomly introduced to prove the robustness of the algorithm, while two quadrotors ( $A_7, A_8$ ) act as false positives, since they are detected by the others but do not communicate any information.

The results of the bearing-only algorithm are in Fig. 4. The large starting error on the distance is due to its random initialization. We start from a large value (around 12 m while the robot distances are around 3 m) to prove that the algorithm is able not only to maintain the right

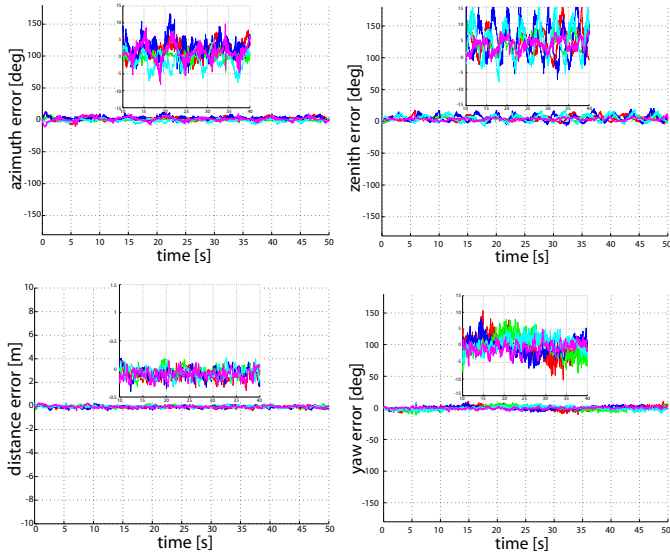


Fig. 5. Bearing+distance algorithm. Errors on azimuth, zenith-distance, distance and yaw estimates for  $A_2, \dots, A_6$  computed by  $A_1$ , with a zoom for  $[10, 40]$  s.

	azimuth[deg]	zenith[deg]	distance[m]	yaw[deg]
bearing only	5.50 (21.87)	6.45 (21.96)	0.13 (1.04)	0.25 (19.61)
$\sigma_d=1.5$ m	2.64 (21.60)	4.75 (26.45)	0.08 (0.87)	0.27 (12.48)
$\sigma_d=1.0$ m	2.32 (21.59)	4.46 (25.73)	0.07 (0.82)	0.32 (20.65)
$\sigma_d=0.3$ m	0.74 (11.99)	2.93 (12.70)	0.04 (0.43)	0.24 (12.45)

Table 1. Mean and maximum errors.

distance but also to retrieve it. The results of the algorithm designed for Scenario II, with 0.5 m standard deviation noise on the distance measurements, are in Fig. 5.

Table 1 shows the mean (maximum) azimuth, zenith, distance and yaw errors w.r.t. the standard deviation of the noise on the distance measurements. The maximum distance error in the bearing only experiment (first row) is considered after the first 5 s, to allow the algorithm to retrieve the initial scale. The values show that the usage of the distance measurements significantly improves the quality of the estimates even when affected by large noise. The two methods obtain comparable results only when the standard deviation of the noise on the distance measurements exceeds 100% of the measures.

The same conclusions can be drawn from the plots (Fig. 6) of the circular error probable, defined as the probability  $p(e_d = \sqrt{e_x^2 + e_y^2 + e_z^2} < d)$  that the radial error  $e_d$  is less or equal to a parameter  $d$ , where  $e_x, e_y, e_z$  are the errors on the estimates. The plots show how the error needed to satisfy a given probability is in general lower including the distance measurements.

See <http://youtu.be/LUCnNC2veOo> for a clip of the experiment.

## 5. CONCLUSIONS

We have presented a decentralized method for 3-D anonymous mutual localization in multi-robot systems. In particular, we have considered two different scenarios, i.e., the use of bearing-only vs. bearing+distance measurements. The latter can be extracted, for instance, from the video

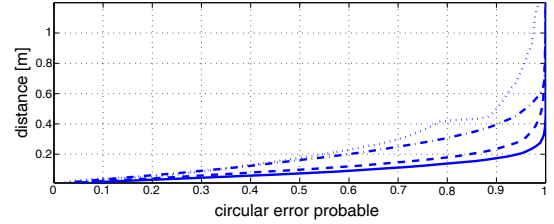


Fig. 6. Circular error probable computed for the bearing-only (dotted) and distance with 0.3 m (solid), 1.0 m (dashed), 1.5 m (dash-dotted) standard deviation noise experiments.

stream of a camera. This device provides very noisy distance measurements, so that they can not be used to retrieve the identities. However, we show how to include them in the estimation process.

Experimentation on a team of UAVs has shown that, in spite of the much larger uncertainty affecting it, the use of distance information improves the performance of the mutual localization system over the bearing-only case. Current work is aimed at implementing the localizer on-board of the UAVs so as to use it for higher level tasks, such as formation control.

## REFERENCES

- Cognetti, M., Stegagno, P., Franchi, A., Oriolo, G., and Bühlhoff, H.H. (2012). 3-D mutual localization with anonymous bearing measurements. In *2012 IEEE Int. Conf. on Robotics and Automation*. St. Paul, MN.
- Fox, D., Burgard, W., Kruppa, H., and Thrun, S. (2000). A probabilistic approach to collaborative multi-robot localization. *Autonomous Robots*, 8(3), 325–344.
- Franchi, A., Oriolo, G., and Stegagno, P. (2009). Mutual localization in a multi-robot system with anonymous relative position measures. In *2009 IEEE/RSJ Int. Conf. on Intelligent Robots and Systems*, 3974–3980. St. Louis, MO.
- Franchi, A., Stegagno, P., and Oriolo, G. (2010). Probabilistic mutual localization in multi-agent systems from anonymous position measures. In *49th IEEE Conf. on Decision and Control*, 6534–6540. Atlanta, GA.
- Howard, A., Mataric, M.J., and Sukhatme, G.S. (2002). Localization for mobile robot teams using maximum likelihood estimation. In *2002 IEEE/RSJ Int. Conf. on Intelligent Robots and Systems*, 434–439. Lausanne, Switzerland.
- Mahony, R., Hamel, T., and Pflimlin, J.M. (2008). Nonlinear complementary filters on the special orthogonal group. *IEEE Trans. on Automatic Control*, 53(5), 1203–1218.
- Martin, P. and Salaün, E. (2010). The true role of accelerometer feedback in quadrotor control. In *2010 IEEE Int. Conf. on Robotics and Automation*, 1623–1629. Anchorage, AK.
- Martinelli, A. (2012). Vision and IMU data fusion: Closed-form solutions for attitude, speed, absolute scale, and bias determination. *IEEE Trans. on Robotics*, 28(1), 44–60.
- Roumeliotis, S.I. and Bekey, G.A. (2002). Distributed multirobot localization. *IEEE Trans. on Robotics*, 18(5), 781–795.
- Stegagno, P., Cognetti, M., Franchi, A., and Oriolo, G. (2011). Mutual localization using anonymous bearing-only measures. In *2011 IEEE/RSJ Int. Conf. on Intelligent Robots and Systems*, 469–474. San Francisco, CA.
- Trawny, N., Zhou, X.S., Zhou, K., and Roumeliotis, S.I. (2010). Inter-robot transformations in 3D. *IEEE Trans. on Robotics*, 26(2), 225–243.
- Zhou, X.S. and Roumeliotis, S. (2011). Determining the robot-to-robot 3D relative pose using combinations of range and bearing measurements (part II). In *2011 IEEE Int. Conf. on Robotics and Automation*, 4736–4743. Shanghai, China.